Charged-Higgs-boson search via heavy-top-quark decay at Fermilab Tevatron collider energy

R. M. Godbole
Department of Physics, University of Bombay, Bombay 400 098, India

D. P. Roy*
Tata Institute of Fundamental Research, Homi Bhabha Road, Bombay 400 005, India

(Received 30 January 1991)

Assuming a top-quark mass of about 150 GeV we analyze the prospects for a charged-Higgs-boson search in top-quark decay at the Fermilab Tevatron upgrade. Universality predicts the relative size of the top decay signal via W boson in different decay channels, and an observable excess over this prediction can be used as a signature for charged-Higgs-boson production. In the charged-Higgs-boson–fermion coupling scheme suggested by minimal supersymmetry and E_6 string-inspired models one expects to see an observable signal up to a charged-Higgs-boson mass of 100 GeV throughout the allowed range of the coupling parameter $\tan\beta$. The absence of such a signal would give an unambiguous charged-Higgs-boson mass limit of 100 GeV. This is not possible however in the alternative coupling schemes of two-Higgs-doublet models.

I. INTRODUCTION

The results from the top-quark-search experiment at the Fermilab Tevatron $\bar{p}p$ collider[1] as well as the B_d-$\bar{B}_d$ mixing data[2] suggest a heavy quark of mass $m_t > 80$ GeV. Further, the radiative correction to W, Z masses suggest a fairly narrow range for m_t with a central value of about 150 GeV.[3] It is also reasonably certain that a top quark of about 150-GeV mass will have an observable signal[4] at the Tevatron upgrade, planned for the early 1990s. Besides providing the first direct evidence for the top quark this will enable one to probe for new particles in the top-quark decay; the large mass of the top quark offers the possibility of carrying on this probe to a hitherto unexplored mass range. In particular there has been a great deal of theoretical and phenomenological interest in one such new particle—i.e., the charged Higgs boson[5] appearing in the two-Higgs-doublet versions of the standard model.[6] The present work is devoted to a systematic study of the prospects for a charged-Higgs-boson search at the Tevatron collider energy. In particular we shall address ourselves to the following questions. (1) Assuming a top-quark mass of 150 GeV, what range of charged-Higgs-boson mass can be probed unambiguously in the sense that it gives an observable signal over the full (allowed) range of the coupling parameter? Nonobservation of this signal would then clearly imply the absence of a charged Higgs particle over this mass range. (2) What are the promising channels for the charged-Higgs-boson signal over the different parts of the coupling-parameter space and what kind of detection efficiencies are required for these channels?

II. TWO-HIGGS-DOUBLET MODEL

The two-Higgs-doublet model[6] contains two SU(2) doublets of complex scalar fields

$$\begin{bmatrix}\phi_1^0\\ \phi_1^-\end{bmatrix}, \quad \begin{bmatrix}\phi_2^+\\ \phi_2^0\end{bmatrix}$$

with the vacuum expectation values (VEV's)

$$\langle\phi_1^0\rangle = v_1/\sqrt{2}, \quad \langle\phi_2^0\rangle = v_2/\sqrt{2}\ . \tag{1}$$

They satisfy the G_F constraint

$$v_1^2 + v_2^2 = v^2 \quad (v = 246\ \text{GeV})\ . \tag{2}$$

A key parameter of the model is the ratio of the VEV's:

$$\tan\beta = v_2/v_1\ . \tag{3}$$

After removing the three Goldstone bosons one is left with five physical Higgs bosons. They are the neutral CP-even states h^0, H^0 and CP-odd state A^0 along with the charged states $H^\pm$. We shall be concerned here only with the charged states, i.e.,

$$H^\pm = \phi_2^\pm \cos\beta - \phi_1^\pm \sin\beta\ . \tag{4}$$

The two-Higgs-doublet model is attractive for several reasons. It is a minimal extension of the standard model in that it adds the fewest new arbitrary parameters. Moreover, it naturally satisfies the constraints of $\rho = 1$ and the absence of flavor-changing neutral currents at the tree level. While the first is guaranteed by the doublet structure of the Higgs boson the second is ensured by choosing the Higgs-boson–fermion couplings so as to satisfy the Glashow-Weinberg theorem.[7] It states that the tree-level flavor changing neutral current mediated by Higgs bosons will be absent if all fermions of a given electric charge have Yukawa coupling to only one Higgs doublet. A very important model automatically satisfying this theorem is the minimal supersymmetric extension of the standard model, where the up-type quarks have Yukawa couplings to one Higgs doublet (ϕ_2 say) while the down-type quarks and charged leptons couple to the oth-

er. This particular two-Higgs-doublet model has received wide attention[6] since it provides the most economical solution to the hierarchy problem of the standard model. Moreover it offers the possibility of explaining the observed quark mass hierarchy $m_c \gg m_s$ and $m_t \gg m_b$ in terms of that of the VEV's $v_2 \gg v_1$. In this model the Yukawa couplings of the physical charged Higgs fields of Eq. (4) to fermions are given in terms of the parameter β as follows:

$$\alpha = \frac{g}{\sqrt{2}M_W} H^+ (\cot\beta\, V_{ij} m_{ui} \bar{u}_i d_{jL} + \tan\beta\, V_{ij} m_{dj} \bar{u}_i d_{jR} + \tan\beta\, m_{lj} \bar{\nu}_j l_{jR}) + \text{H.c.} , \quad (5)$$

where V_{ij} are the Kobayashi-Maskawa (KM) matrix elements. One has identical charged-Higgs-boson couplings to fermions in E_6 superstring-inspired models as well. The main phenomenological difference between the minimal-supersymmetry (SUSY) and E_6 models is that while the former predicts a mass bound $m_H > m_W$ (Ref. 6) the latter gives a less restrictive bound[8] $m_H > 53$ GeV.

In addition to Eq. (5), there are three other combinations of charged-Higgs-boson couplings to fermions allowed by the Glashow-Weinberg theorem[9]—i.e., where the $T_3 = -\frac{1}{2}$ quarks or leptons or both are assumed to have Yukawa couplings to ϕ_2 instead of ϕ_1. They correspond to replacing $\tan\beta$ by $-\cot\beta$ in the second or third or both the terms in Eq. (5). In the last case all the fermions couple to the same Higgs doublet as in the minimal Higgs model while the other doublet decouples completely from the fermion sector (due to some discrete symmetry).[6] In the other two cases the $T_3 = -\frac{1}{2}$ quarks and leptons have Yukawa couplings to different Higgs doublets. There is no theoretical motivation for this as far as we know. In the present analysis we shall concentrate on the charged-Higgs-boson–fermion coupling scheme of Eq. (5) in view of the considerable theoretical interest behind it. We shall however discuss how the results change when one moves over to the alternative schemes. In particular, we shall see that one expects an unambiguous charged-Higgs-boson signal over a significant mass range for the coupling scheme of Eq. (5) but not for any of the alternative schemes.

There are already some constraints on the charged-Higgs-boson mass[10] and the coupling parameter $\tan\beta$.[9,11] (1) A charged-Higgs-boson search at the CERN e^+e^- collider LEP at the ALEPH Collaboration[10] has given a lower-mass bound of about 40 GeV; the exact value varies between 35 and 43 GeV depending on the value of $\tan\beta$. (2) Validity of perturbation theory implies an upper bound on the charged-Higgs-boson–fermion Yukawa couplings of Eq. (5). In particular the coupling proportional to m_t, appearing in the first term of Eq. (5), can be potentially large. Requiring this to be bounded by the size of the strong coupling $\sqrt{4\pi\alpha_s}$ ($\simeq 1.2$) or equivalently $\Gamma(t \to bH^+) \lesssim \frac{1}{2} m_t$ gives[9,11]

$$\tan\beta > m_t/600 \text{ GeV } (\simeq \tfrac{1}{4}) . \quad (6)$$

The size of the tbH^+ coupling has also been constrained by the contribution of the H^+ exchange box diagram to B_d-$\bar{B}_d$ mixing or the corresponding loop diagrams to $b \to s\gamma$ decay and the ϵ'/ϵ ratio. Thus a lower bound of $\tan\beta > 0.3$–0.4 has been obtained in Ref. 9, for $m_t = 150$ GeV and $m_H \leq 100$ GeV. (3) Applying an analogous perturbative limit for the coupling proportional to m_b, appearing in the second term of Eq. (5), gives an upper bound on $\tan\beta$,[11] i.e.,

$$\tan\beta < 600 \text{ GeV}/m_b \ (\simeq 120) . \quad (7)$$

One should note that there is no such upper bound in the alternative coupling scheme where all the fermions have Yukawa couplings to the same Higgs doublet—i.e., all the terms in Eq. (5) are proportional to $\cot\beta$. In contrast the lower bound is valid for all the alternatives since it is controlled by the first term of Eq. (5), which remains the same in each case. In view of the above-mentioned bounds on m_H and $\tan\beta$, the region of phenomenological interest is $m_H > 40$ GeV and $\tan\beta = 0.5 - 100$. We shall restrict our analysis to this region. It may be noted that this range of charged-Higgs-boson mass is also of theoretical interest to the minimal-SUSY and E_6 superstring-inspired models. We should add that there is a stronger bound on $\tan\beta$ (≥ 1.6) from the LEP constraints on Higgs-boson masses,[10] which is, however, highly model dependent and hence shall not be used here.

III. CHARGED-HIGGS-BOSON SIGNAL VERSUS *W*-BOSON BACKGROUND IN TOP-QUARK DECAY

The size of the charged-Higgs-boson signal vis a vis the W-boson background is controlled by the relative decay widths of $t \to bH^+$ and $t \to bW^+$. In the approximation of a diagonal KM matrix, one gets[12]

$$\Gamma_{t\to bW^+} = \frac{g^2}{64\pi m_W^2 m_t} \lambda^{1/2}\left(1, \frac{m_b^2}{m_t^2}, \frac{m_W^2}{m_t^2}\right)[m_W^2(m_t^2+m_b^2) + (m_t^2-m_b^2)^2 - 2m_W^4] . \quad (8)$$

The corresponding decay width into charged Higgs boson can be calculated from Eq. (5), i.e.,

$$\Gamma_{t-bH^+} = \frac{g^2}{64\pi m_W^2 m_t} \lambda^{1/2}\left(1, \frac{m_b^2}{m_t^2}, \frac{m_H^2}{m_t^2}\right)[(m_t^2\cot^2\beta + m_b^2\tan^2\beta)(m_t^2+m_b^2-m_H^2) + 4m_t^2 m_b^2] . \quad (9)$$

Thus one gets the branching fraction

$$B(t\to bH^+)=\Gamma_{t\to bH^+}/(\Gamma_{t\to bH^+}+\Gamma_{t\to bW^+}) . \quad (10)$$

From Eq. (5) one can also calculate the two significant decay widths of charged Higgs bosons: i.e.,

$$\Gamma_{H^+\to\tau^+\nu}=\frac{g^2 m_H}{32\pi m_W^2} m_\tau^2 \tan^2\beta , \quad (11)$$

$$\Gamma_{H^+\to c\bar{s}}=\frac{3g^2 m_H}{32\pi m_W^2}(m_c^2\cot^2\beta+m_s^2\tan^2\beta) , \quad (12)$$

and the branching fraction

$$B(H^+\to\tau^+\nu)=m_\tau^2\tan^2\beta/3(m_c^2\cot^2\beta+m_s^2\tan^2\beta)+m_\tau^2\tan^2\beta , \quad (13)$$

where the factor 3 is the quark color factor and we have neglected a kinematic factor of $(1-m_\tau^2/m_H^2)^2$ in Eq. (11) along with a similar factor in Eq. (12).[13] The corresponding branching fractions for W decay are of course given by the universality of W coupling to leptons and quarks; i.e., $\simeq\frac{1}{9}$ for each lepton species and $\simeq\frac{2}{3}$ into hadrons. One should note the striking difference between the two sets of branching fractions. We shall come back to this point later on. Like W the charged Higgs boson has also to be identified through its leptonic (i.e., τ) decay in view of the large QCD background for the hadronic channel.

Figure 1 shows the branching fraction of $t\to bH^+$ as a function of $\tan\beta$ for several values of charged-Higgs-boson mass in the range 60–120 GeV. For $m_H\sim m_W$ the charged-Higgs-boson branching fraction is comparable to that into the W boson for $\tan\beta\sim 1$; however, it has a very strong dependence on $\tan\beta$. At the two extreme values of this parameter ($\tan\beta\simeq 0$ and $\simeq 100$), the $t\to bH^+$ becomes the dominant decay mode since the corresponding coupling becomes large as we have seen before. On the other hand this branching fraction becomes very small in the region $\tan\beta\simeq 5.5$. This is due to a deep minimum in the $t\to bH^+$ partial width of Eq. (9) at

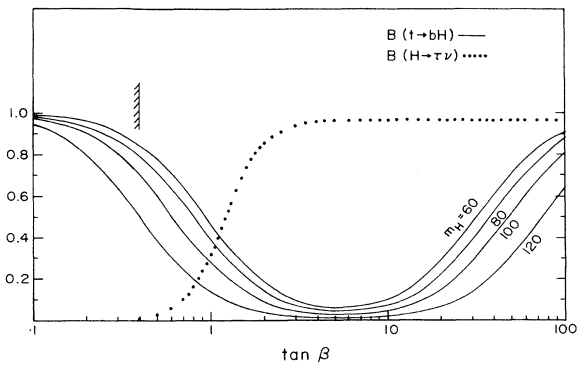

FIG. 1. The branching fraction of top-quark decay into charged Higgs boson for $m_t=150$ GeV and $m_H=60$–120 GeV. The branching fraction of charged-Higgs-boson decay into τ lepton is also shown (dotted line). The allowed range of $\tan\beta$ ($\gtrsim 0.4$) is indicated by the hatched line in all the figures.

$$\tan\beta=\sqrt{m_t/m_b}\simeq 5.5 . \quad (14)$$

Figure 1 also shows the branching fraction for charged-Higgs-boson decay $H^+\to\tau^+\nu$, calculated with $m_\tau=1.8$ GeV, $m_c=1.5$ GeV, and $m_s=0.2$ GeV. However, it is not sensitive to the exact value of the strange-quark mass. It rises steadily from 0 to nearly 1 as $\tan\beta$ increases from 0 to 2 and remains practically constant thereafter. It is the product of the above two branching fractions that controls the size of the observable charged-Higgs-boson signal. It is evident from Fig. 1, that the $\tan\beta\simeq 0$ region would be bad not only for the charged Higgs boson but for the top-quark search as well, since the dominant decay mode is into the unobservable channel $t\to bH^+\to bc\bar{s}$. Fortunately the worst part is disallowed by the constraints on tbH coupling from perturbation theory as well as the low-energy processes.[9,11] Of the allowed part of $\tan\beta$ space, the potentially problematic regions are $\tan\beta\simeq 0.5$ and $\tan\beta\sim 5$ where the $H^+\to\tau^+\nu$ and $t\to bH^+$ branching fractions are small, respectively. Fortunately the small value of one branching fraction is partly compensated by the large value of the other. Consequently the size of the charged-Higgs-boson signal will be at least comparable to the W-boson background throughout the allowed range of $\tan\beta$ for $m_H\sim m_W$.

The basis process of interest is $t\bar{t}$ production through gluon-gluon or quark-antiquark fusion followed by their decay into charged-Higgs-boson or W-boson channels; i.e.,

$$gg(q\bar{q})\to t\bar{t}\to\bar{b}H^-(W^-) \to bH^+(W^+) . \quad (15)$$

This is the lowest-order QCD process for $t\bar{t}$ production, which is known to be adequate for the large quark mass of our interest. Besides we will be primarily interested in the relative contribution from the H and W channels from which the $t\bar{t}$ production cross section factors out. To avoid QCD background, at least one of the two charged bosons is required to decay into the τ channel; i.e.,

$$H^+(W^+)\to\tau^+\nu_\tau , \quad (16)$$

$$H^-(W^-)\to\bar{q}q' , \quad (17)$$

or vice versa. Finally the τ is to be observed in its hadronic or muonic decay

$$\tau\to\nu_\tau\bar{q}q' , \quad (18)$$

$$\tau\to\nu_\tau\nu_\mu\mu , \quad (19)$$

as a narrow jet or a relatively soft muon, accompanied by a large missing p_T.

We have computed the above $t\bar{t}$ production cross section and sequential decay for the $\bar{p}p$ collider energy of 2 TeV and integrated luminosity of 100 pb^{-1}, as expected for the Tevatron upgrade. A luminosity of several hundred pb^{-1}, which seems plausible now, will help to compensate for the detection (in)efficiency factors. The basic $t\bar{t}$ production cross section of Eq. (15) is convoluted with the gluon (quark) densities of Ref. 14. This corresponds to a three-dimensional integration. Since every 2-

(3-)body decay corresponds to a 2- (5-)dimensional integration, we have a 13 dimensional integration for the sequential decay involving H^+H^-. The corresponding number is 15 for the W^+W^- channel, since the two-body decays of Eqs. (15)–(17) have to be handled as three-body decays

$$t \xrightarrow{W^+} b\tau^+\nu_\tau \qquad \bar{t} \xrightarrow{W^-} \bar{b}\bar{q}q' \tag{20}$$

to take care of the W polarization. Thus one has a total of 16- (18-)dimensional integration for the $H^+H^-(W^+W^-)$ channel. These are done, of course, using a Monte Carlo program.

We have found that for $m_H \leq 100$ GeV the charged-Higgs-boson contribution is at least as large as the W-boson contribution over the allowed $\tan\beta$ range, apart from a gap around $\tan\beta \sim 5$. This corresponds to the region in Fig. 1, where the $t \to bH^+$ branching fraction has a minimum. However, this gap can be closed by considering the decay of both the charged bosons into τ leptons. Moreover, the size of the charged-Higgs-boson contribution remains sufficiently large for observation over the entire range of $\tan\beta$. But it is very hard to distinguish the charged-Higgs-boson signal from the W-boson background on the basis of their kinematic distributions. Although the two charged bosons have different spins the resulting difference in the observable kinematic distributions are very marginal. Moreover for the mass range of our interest, $m_H = 60-100$ GeV, the mass difference between H and W is not large enough to give a clear kinematic distinction. The best way to separate the H and W contributions is to look for the departure from universality as suggested by the distinctive charged-Higgs-boson couplings to quarks and different species of leptons—in particular its preferential coupling to the τ lepton. This results in the charged-Higgs-boson branching fractions into these channels being very different from those of the W boson as we have seen in the beginning of this section.

IV. CHARGED-HIGGS-BOSON DETECTION THROUGH DEPARTURE FROM UNIVERSALITY IN TOP-QUARK DECAY

We shall see now that the departure from universality in the different $t\bar{t}$ decay channels provides an effective signature for charged-Higgs-boson production. This can be exploited to give an observable signal for charged-Higgs-boson production up to $m_H \simeq 100$ GeV throughout the allowed range of $\tan\beta$. We shall proceed as follows. In a given channel of $t\bar{t}$ decay the W background corresponds to the WW contribution while the charged-Higgs-boson signal corresponds to the $(HH+WH)$ contribution. The dilepton channel (e^+e^-, $\mu^+\mu^-$, $e^\pm\mu^\mp$) for $t\bar{t}$ decay provides an unambiguous normalization for the W background because of the negligible charged-Higgs-boson couplings to these leptons. Then universality simply predicts the size of the W background in any other channel relative to the above; and a sizeable excess over this prediction will constitute a signal for charged-Higgs-boson production. We shall assume a working definition for an observable signal as one corresponding to $\gtrsim 10$ signal events and a signal/background ratio ≥ 1.

Figures 2–6 show the predicted size of the W background and the charged-Higgs-boson signal in different channels of $t\bar{t}$ decay for

$$m_t = 150 \text{ GeV}, \quad \sqrt{s} = 2 \text{ TeV}, \quad \int \mathcal{L}\, dt = 100 \text{ pb}^{-1}. \tag{21}$$

The predictions are shown for two values of the charged-Higgs-boson mass ($m_H = 60$, 100 GeV) and for the full allowed range of the coupling parameter ($\tan\beta = 0.5-100$). It should be noted that in each figure the peak value of the W background at $\tan\beta \simeq 5$ is approximately the same as the prediction in the absence of a charged Higgs boson.

A. Hard dipleton channel

In Fig. 2 the dotted lines show the predicted W background for the hard dilepton channel with $p^T_{e,\mu} > 15$ GeV, for which there is no charged-Higgs-boson contribution. The prediction of a model without the charged Higgs boson can be read off from the peak value of the curves. Compared to this value the prediction of a model with charged Higgs bosons can be significantly smaller for certain ranges of m_H and $\tan\beta$. However, a similar variation could also arise from the uncertainties in the QCD prediction and the top-quark mass. Therefore any mismatch between the observed event rate and the peak value of the prediction should not be regarded as a charged-Higgs-boson signal. Instead the observed event rates should be used to normalize the W background, so that the W background in all other channels is unambiguously predicted via universality. It should be emphasized here that while the predicted W background in all the channels shows substantial variation with m_H and $\tan\beta$, their relative magnitudes are independent of these parameters and unambiguously predicted via universality. A sizeable excess (by $\gtrsim 100\%$) over the predicted value in any of these

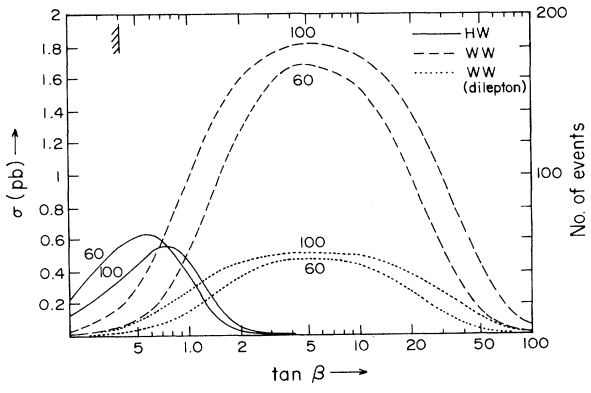

FIG. 2. The charged-Higgs-boson signal (solid line) and W-boson background (dashed line) for $m_H = 60$ and 100 GeV in the hard-muon + multijet channel of $t\bar{t}$ decay. The W background in the hard dilepton channel is shown (dotted line) for normalization. The cuts are given in Table I.

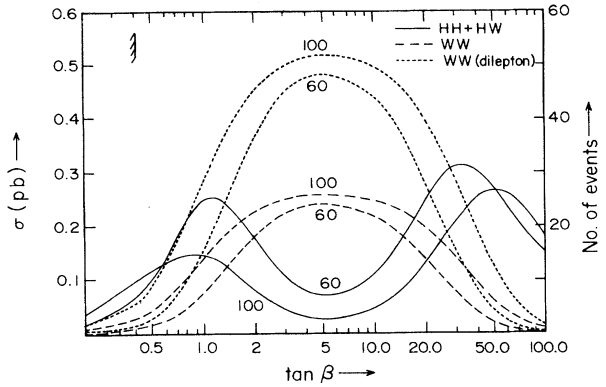

FIG. 3. The charged-Higgs-boson signal (solid line) and W-boson background (dashed line) for $m_H = 60$ and 100 GeV in the soft-muon + multijet channel of $t\bar{t}$ decay. The W background in the hard-dilepton channel is shown (dotted line) for normalization. The cuts are given in Table I.

channels can be regarded as a signal for charged-Higgs-boson contribution.

B. Hard-muon + multijet channel

It corresponds to muonic decay of one charged boson (W) and hadronic decay of the other (W,H). Figure 2 shows the charged-Higgs-boson signal (WH) along with the W background (WW) for $p_\mu^T > 15$ GeV and the following cuts on the jet parameters:

$$N_j \geq 2, \quad p_{j1}^T > 40 \text{ GeV}, \quad p_{j2}^T > 30 \text{ GeV} . \tag{22}$$

The cuts on the jet parameters have practically no effect on the above signal or background (increasing the p_{j2}^T cut to 40 GeV would reduce them by $\simeq 20\%$). But they help to suppress the background from W + QCD jets, as we shall see later. One sees from Fig. 2 that this channel provides an observable charged-Higgs-boson signal up to $m_H = 100$ GeV only over a limited range of

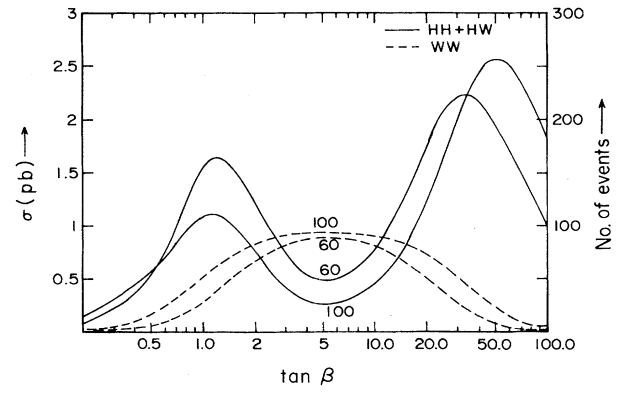

FIG. 4. The charged-Higgs-boson signal (solid line) and W-boson background (dashed line) for $m_H = 60$ and 100 GeV in the τ-jet + multijet channel of $t\bar{t}$ decay. The cuts are given in Table I.

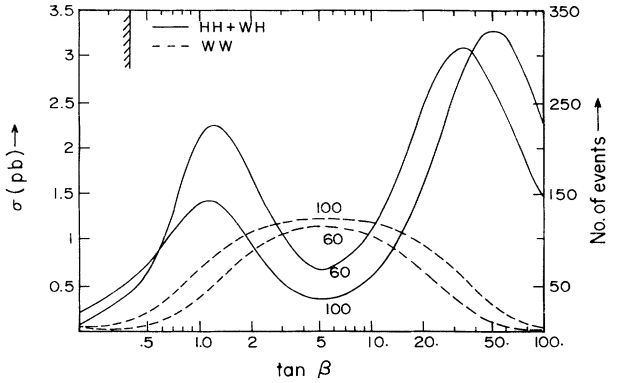

FIG. 5. The charged-Higgs-boson signal (solid line) and W-boson background (dashed line) for $m_H = 60$ and 100 GeV in the large-missing-p_T + multijet channel of $t\bar{t}$ decay. The cuts are given in Table I.

$\tan\beta = 0.5-0.7$. The reason for the relatively modest size of the charged-Higgs-boson signal is, of course, the absence of the HH contribution in this channel. To include this contribution one must look at the channels which correspond to τ decay of at least one of the charged bosons. We consider a few such channels below.

C. Soft-muon + multijet channel

This corresponds to τ decay of one of the charged bosons followed by its muonic decay, while the other decays into hadrons [Eqs. (16), (17), and (19)]. Of course one has to add the contribution from the low p_T tail of the muons coming from the direct W decay. Figure 3 shows the resulting charged-Higgs-boson signal along with the W background for $p_\mu^T = 5-15$ GeV and the jet cuts of Eq. (22). The W background for the hard dilepton channel, to be used for normalization, is also shown for convenience. As we see from Fig. 3, this channel provides an observable charged-Higgs-boson signal upto $m_H = 100$ GeV over a somewhat wider range of $\tan\beta$, i.e., $\tan\beta = 0.5-1$ and > 25. Nonetheless there is a huge gap over the range $1 < \tan\beta < 25$. This channel has two limitations—(1) sig-

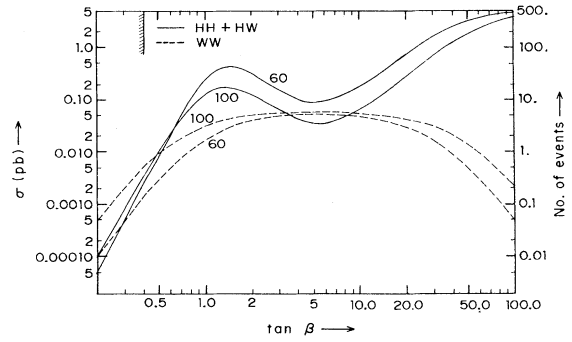

FIG. 6. The charged-Higgs-boson signal (solid line) and W-boson background (dashed line) for $m_H = 60$ and 100 GeV in the two-τ-jet channel of $t\bar{t}$ decay. The cuts are given in Table I.

nal size is small due to the small muonic branching fraction of τ ($\simeq 0.18$) and (2) the contribution to low p_T muons from direct W decay roughly doubles the size of the background.

D. τ-jet + multijet channel

This corresponds to τ decay of one of the charged bosons and hadronic decay of the other, followed by the hadronic decay of τ [Eqs. (16)–(18)]. The narrow jet coming from τ decay (τ jet) is expected to provide a tag for τ. The identification of the τ jet seems to be facilitated in the presence of a sizable missing p_T (≥ 20 GeV).[15] We have therefore imposed the cuts p^T (τ jet) > 10 GeV, $p^T_{\rm miss} > 20$ GeV and those of Eq. (22) for the remaining jets. The resulting charged-Higgs-boson signal and W background are shown in Fig. 4. The size of the signal is larger compared to the previous channel due to the large hadronic branching fraction of τ ($\simeq 0.64$); and the signal to background ratio is also somewhat larger. It provides an observable charged-Higgs-boson signal up to $m_H = 100$ GeV over a major part of the tanβ space—i.e., except the range $2 < \tan\beta < 15$.

E. Missing-p_T + multijet channel

This corresponds to τ decay of one of the charged bosons and hadronic decay of the other, followed by τ decay into both hadronic and leptonic channels [Eqs. (16)–(19)]. The multiple neutrino emission in these processes gives rise to a sizable missing p_T, which can be used as an effective signature for τ. We assume that the $W \to e\nu, \mu\nu$ events would be recognized by the hard lepton and hence do not include their contribution. Figure 5 shows the charged-Higgs-boson signal and W background for $p^T_{\rm miss} > 40$ GeV along with the jet cut of Eq. (22). The missing-p_T cut costs about 30% of the signal. The size of the signal and the signal-to-background ratio for this channel are very similar to the previous one. As in the previous case it also provides an observable charged-Higgs-boson signal up to $m_H = 100$ GeV throughout the allowed tanβ range except $2 < \tan\beta < 15$. In order to close this gap one has to look at a channel corresponding to τ decay of both the charged bosons, as we see below.

F. Two-τ-jet channel

This corresponds to τ decay of both the charged bosons followed by hadronic decay of both the τ's. The cross sections have been calculated with a p_T cut of 10 GeV for both the τ jets along with a missing-p_T cut of 20 GeV. The resulting charged-Higgs-boson signal and the W background are shown in Fig. 6. We see now that there is practically no gap left in the tanβ space. The two-τ-jet channel provides an observable charged-Higgs-boson signal up to $m_H = 100$ GeV for essentially the entire range of allowed tanβ values. Only at the extreme end of tan$\beta = 0.5$–0.7 does the signal fall below the 10-event level. Thus the two-τ-jet channel provides the most promising channel for charged-Higgs-boson search in heavy top decay at the Tevatron upgrade. It depends strongly, however, on the efficiency of τ-jet detection. While the signal-to-background ratio is not sensitive to this efficiency factor the size of the signal is evidently very sensitive. Of course a loss of signal size due to this (in)efficiency factor can be compensated for if one has an integrated luminosity significantly larger than 100 pb^{-1} at the Tevatron upgrade, as mentioned before.

G. W+QCD jets background

This is known to be the most serious background for the heavy top-quark signal in lepton-plus-multijet channels. Several prescriptions for suppressing this background have been suggested using the fact that the QCD jets are generally soft or collinear. We have found that the most efficient way of suppressing this background is the straight p_T cut on the jets. Increasing the p_T cut for the two hardest jets from 10 to 40 GeV reduces this background by a little over an order of magnitude while reducing the top-quark signal by only 20%. We have estimated this background using the formalism of Ref. 16 for

$$N_j = 2 \text{ and } p^T_{j1}, p^T_{j2} > 40 \text{ GeV} \tag{23}$$

for the multijet channels $B - E$ above. The background cross sections are 5 pb for the multijet channel with hard lepton (Fig. 2) and about 3 pb each for the multijet channels with τ jet (Fig. 4) and missing p_T (Fig. 5). These are still large compared to the top-quark signal shown in these figures, particularly after its splitting into the charged-Higgs-boson and W channels. Moreover, with the above jet-p_T cuts the kinematic distributions of background are very similar to those of the top-quark signal (including the two-jet invariant-mass distribution), so that it cannot be significantly reduced by any more kinematic cuts. The best way of doing this is to increase the number of jets to $N_j \geq 3$. As noted by several authors[17] before, this would reduce the background by a factor of 5 or more while removing only 20% of the top-quark signal. This level of background contribution to the multijet channels with τ jet or missing p_T (i.e., ~ 0.6 pb) will be tolerable compared to the cross sections of our interest, shown in Figs. 4 and 5.

V. SUMMARY AND CONCLUSION

We have seen how one can search for charged-Higgs-boson in heavy-top-quark decay at the Tevatron upgrade, by comparing the size of the $t\bar{t}$ signal in different decay channels. We have assumed a top-quark mass of 150 GeV and the charged-Higgs-boson–fermion coupling scheme [Eq. (5)] suggested by the minimal-SUSY and the E_6 superstring-inspired models; and investigated the charged-Higgs-boson discovery potential of various channels as a function of the charged-Higgs-boson mass and coupling parameter tanβ. The results are summarized in Table I, which shows that different channels can probe charge-Higgs-boson mass up to 100 GeV over different ranges of the tanβ space. The most promising channels are the multijet channels accompanied by a τ jet or a siz-

TABLE I. Charged-Higgs-boson search potential of various top-quark decay channels for $m_t = 150$ GeV. Each channel can probe charged-Higgs-boson mass up to 100 GeV over the tanβ range indicated.

Channel	Basic cuts (GeV)	tanβ range	Figs.
A. Hard dilepton	$p^T_{\mu,e} > 15$	Background norm.	2,3
B. Hard muon + multijet	$p^T_\mu > 15; N_j \geq 2, p^T_{j1} > 40, p^T_{j2} > 30$	0.5–0.7	2
C. Soft muon + multijet	$p^T_\mu = 5-15; N_j \geq 2, p^T_{j1} > 40, p^T_{j2} > 30$	0.5–1 & >25	3
D. τ jet + multijet	$p^T_{\tau\,\text{jet}} > 10, p^T_{\text{miss}} > 20; p^T_{j1} > 40, p^T_{j2} > 30$	0.2–2 & >15	4
E. Missing p_T + multijet	$p^T_{\text{miss}} > 40; p^T_{j1} > 40, p^T_{j2} > 30$	0.2–2 & >15	5
F. Two τ jets	$p^T_{\tau\,\text{jet}} > 10, p^T_{\text{miss}} > 20$	0.7<	6

able missing p_T and the two-τ-jet channel. The first two can probe charged-Higgs-boson masses up to 100 GeV over a major part of the allowed tanβ space (i.e., for tan$\beta < 2$ and > 15) while the last channel can do this for essentially the whole of the allowed tanβ space.

If there is a charged-Higgs-boson signal one can determine the mass m_H and the coupling parameter tanβ by comparing the size of the signals in different channels. While the size of the signals in all the channels increases with decreasing m_H, their relative size depends sensitively on the tanβ parameters as we see from Figs. 2–6. Moreover, one can get reasonable constraints on m_H from some of the kinematic distributions. We have checked that the transverse mass of the τ-jet and missing-p_T system is a good kinematic variable for this purpose. If, on the other hand, there is no observable signal in the above-mentioned channels one can raise the charged-Higgs-boson mass limit from 40 to 100 GeV unambiguously—i.e., without any *ad hoc* assumption about the tanβ parameter. One should note that this range of charged-Higgs-boson mass is of interest to the minimal-SUSY and E_6 superstring-inspired models.

Finally let us briefly discuss what happens in the alternative charged-Higgs-boson–fermion schemes described in Sec. II. In none of these alternative schemes does one expect to see an unambiguous Higgs signal—i.e., there is always a gap in the allowed tanβ space. The reasons are the following.

(1) Models where both up- and down-type quarks have Yukawa couplings to the same Higgs doublet correspond to replacing tanβ by $-\cot\beta$ in the second term of Eq. (5) and hence in Eq. (9). Consequently the $t \to bH^+$ branching fraction decreases continuously with increasing tanβ, so that the top quark essentially decouples from the charged Higgs boson over a large part of the allowed tanβ space.

(2) In the model with the same charged-Higgs-boson coupling in the quark sector but with the charged leptons coupling to ϕ_2 instead of ϕ_1, one has to replace tanβ by $-\cot\beta$ in the third term of Eq. (5) and hence in Eq. (11). Consequently the region of small $t \to bH^+$ branching fraction in Fig. 1 (tanβ=3–10) corresponds to small $H^+ \to \tau^+ \nu$ branching fraction as well, so that one cannot get an observable signal. Moreover, the $H^+ \to \tau^+ \nu$ branching fraction essentially vanishes for tan$\beta > 10$, so that the charged-Higgs-boson decay becomes practically unobservable.

Thus for each of these alternative schemes there are no observable charged-Higgs-boson signals over large parts of the allowed tanβ space.[18] It is the distinctive correlation between the three charged-Higgs-boson coupling terms in Eq. (5) that ensures an observble charged-Higgs-boson signal in this model throughout the allowed tanβ space.

ACKNOWLEDGMENTS

We wish to thank Dr. Sourendu Gupta for his collaboration in writing the W+QCD jets program. Thanks are also due to Dr. Chara Petridou for communication on the subject of τ-jet detection efficiency. Discussions with Dr. Probir Roy are gratefully acknowledged. One of the authors (R.M.G.) acknowledges financial support by the Board of Research in Nuclear Sciences, India.

*Address from 1 February 1991 to 31 January 1992: Theory Division, CERN, Geneva, Switzerland.

[1]CDF Collaboration, F. Abe *et al.*, Phys. Rev. Lett. **64**, 142 (1990); Phys. Rev. D **43**, 664 (1991); L. Pondrom, in *Proceedings of the 25th International Conference on High Energy Physics*, Singapore, 1990, edited by K. K. Phua and Y. Yamaguchi (World Scientific, Singapore, 1991).

[2]G. Altarelli and P. Franzini, Z. Phys. C **39**, 271 (1988); P. Franzini, Phys. Rep. **173**, 1 (1989), and references therein.

[3]J. Ellis and G. Fogli, Phys. Lett. B **232**, 139 (1989); P. Langacker, Phys. Rev. Lett. **63**, 1920 (1989); F. Halzen and D. A. Morris, Phys. Lett. B **237**, 107 (1990); E. Jenkins and A. V. Manohar, *ibid.* **237**, 259 (1990).

[4]Sourendu Gupta and D. P. Roy, Z. Phys. C **39**, 417 (1988); H. Baer, V. Barger, and R. J. N. Phillips, Phys. Rev. D **39**, 3310 (1989).

[5]See, e.g., A. C. Bawa, C. S. Kim, and A. D. Martin, Z. Phys. C **47**, 75 (1990); R. M. Barnett *et al.*, in Proceedings of the 1990 Summer Study on High Energy Physics, Snowmass, Colorado (unpublished).

[6]For a review of minimal Higgs sector and its extensions, see J. F. Gunion, H. E. Haber, G. L. Kane, and S. Dawson, *The Higgs Hunter's Guide* (Addison-Wesley, Reading, MA, 1990); H. E. Haber, in *Phenomenology of the Standard Model and*

Beyond, Workshop on High Energy Physics Phenomenology, Bombay, India, 1989, edited by D. P. Roy and Probir Roy (World Scientific, Singapore, 1989), p. 197.

[7]S. Glashow and S. Weinberg, Phys. Rev. D **15**, 1958 (1977); E. A. Paschos, *ibid*. **15**, 1966 (1977).

[8]J. L. Hewett and T. L. Rizzo, Phys. Rep. **183**, 193 (1989).

[9]V. Barger, J. L. Hewett, and R. J. N. Phillips, Phys. Rev. D **41**, 3421 (1990); J. L. Hewett, Wisconsin University Report No. MAD/PH/565 (unpublished).

[10]ALEPH Collaboration, D. Decamp *et al.,* Phys. Lett. B **241**, 623 (1990); OPAL Collaboration, M. Akrawy *et al., ibid*. **242**, 299 (1990); DELPHI Collaboration P. Aarnio *et al., ibid.* **241**, 449 (1990); L3 Collaboration, S. Ting *et al.,* in *Proceedings of the 25th International Conference on High Energy Physics* (Ref. 1).

[11]A. Buras, P. Krawczyk, M. E. Lautenbacher, and C. Salazar, Nucl. Phys. **B337**, 284 (1990); J. F. Gunion and B. Grzadkowski, Phys. Lett. B **243**, 301 (1990).

[12]V. Barger and R. J. N. Phillips, Phys. Rev. D **41**, 884 (1990).

[13]We have checked that the above expressions for the partial widths agree with the corresponding ones of Ref. 12, apart from a small sign error in their expression for $\Gamma_{t\to bW^+}$.

[14]M. Glück, F. Hoffman, and E. Reya, Z. Phys. C **13**, 119 (1982).

[15]C. Petridou (private communication).

[16]R. Kleiss and W. J. Stirling, Nucl. Phys. **B262**, 235 (1985).

[17]W. T. Giele and W. J. Stirling, Nucl. Phys. **B343**, 14 (1990); V. Barger, J. Ohnemus, and D. Zeppenfeld, Phys. Rev. Lett. **62**, 1971 (1989); Phys. Rev. D **40**, 2888 (1989); **40**, 1715(E) (1990).

[18]The same is true for the two-Higgs-doublet model of Ref. 19, which circumvents Glashow-Weinberg theorem by imposing a discrete symmetry so that the tree-level flavor-changing neutral currents are naturally suppressed below their experimental limits.

[19]A. S. Joshipura and S. D. Rindani, Physical Research Laboratory, Navrangpura, Ahmedabad, India, Report No. TH/90-15 and 16, 1990 (unpublished).